JOURNAL OF VIROLOGY, Dec. 2002, p. 11853–11865 Vol. 76, No. 23
0022-538X/02/$04.00+0 DOI: 10.1128/JVI.76.23.11853–11865.2002

RNA Incorporation Is Critical for Retroviral Particle Integrity after Cell Membrane Assembly of Gag Complexes

Shainn-Wei Wang and Anna Aldovini*

Department of Medicine, Children's Hospital, and Department of Pediatrics, Harvard Medical School, Boston, Massachusetts 02115

Received 17 April 2002/Accepted 22 August 2002

The nucleocapsid (NC) domain of retroviruses plays a critical role in specific viral RNA packaging and virus assembly. RNA is thought to facilitate viral particle assembly, but the results described here with NC mutants indicate that it also plays a critical role in particle integrity. We investigated the assembly and integrity of particles produced by the human immunodeficiency virus type 1 M1-2/BR mutant virus, in which 10 of the 13 positive residues of NC have been replaced with alanines and incorporation of viral genomic RNA is virtually abolished. We found that the mutations in the basic residues of NC did not disrupt Gag assembly at the cell membrane. The mutant Gag protein can assemble efficiently at the cell membrane, and viral proteins are detected outside the cell as efficiently as they are for the wild type. However, only ~10% of the Gag molecules present in the supernatant of this mutant sediment at the correct density for a retroviral particle. The reduction of positive charge in the NC basic domain of the M1-2/BR virus adversely affects both the specific and nonspecific RNA binding properties of NC, and thus the assembled Gag polyprotein does not bind significant amounts of viral or cellular RNA. We found a direct correlation between the percentage of Gag associated with sedimented particles and the amount of incorporated RNA. We conclude that RNA binding by Gag, whether the RNA is viral or not, is critical to retroviral particle integrity after cell membrane assembly and is less important for Gag-Gag interactions during particle assembly and release.

The Gag proteins and viral RNA are the main structural components of a retroviral particle (reviewed in reference 51). The Gag proteins, which are crucial to viral assembly and release, are synthesized initially as a precursor polyprotein. This precursor assembles with the viral RNA at areas of the plasma membrane that are lipid rich and have a density that is higher than that observed for rafts, probably because of the presence of the Gag complexes (32, 43, 52). These raft-like microdomains are called barges (32). During or after budding, the virion undergoes a maturation process, during which the Gag polyprotein is cleaved by the viral protease (PR) into the subenvelope matrix shell (MA), the central capsid shell (CA), the nucleocapsid core protein (NC), p6, and two small spacer peptides (SP1 and SP2) (22, 51). This proteolytic processing is not required for the assembly process, as formation and release of immature virus particles can be observed in the absence of an active protease (51). The result of Gag processing is the maturation of the virion with the condensation of its viral core, which is composed of at least CA, NC, and the viral RNA (1, 20).

Three major regions of the Gag polyprotein, termed M, I, and L domains for membrane binding, interaction, and late budding, respectively, are required for retroviral particle assembly and release (4, 9, 21, 22, 24, 44). A portion of the I domain maps in the NC protein, which in human immunodeficiency virus type 1 (HIV-1) consists of at least the first 14 amino acids of NC (49). This portion of Gag is involved in multiple functions during the retroviral life cycle, including RNA binding, assembly, and chaperone activity during reverse transcription (reviewed in references 13, 19, and 48). The two most striking features of NC are the presence of two zinc binding motifs and a high content of basic residues, which are important for the RNA binding properties of this protein (13, 46). Deletions in the NC domain or of the entire NC result in severe viral assembly defects (7, 14, 16, 21, 23, 26, 28, 33, 53). In addition, some investigators have reported a significant reduction in assembly of the basic residues of NC for mutants (11, 15). However, defects in the assembly process are rarely observed for most zinc finger mutants (14, 26, 28). Mutations in the two zinc binding motifs or in the basic residues significantly reduce RNA incorporation in vivo and RNA binding of the mutant proteins in vitro (5, 6, 12, 25, 44, 45, 47, 50, 54). The substitutions of basic residues in these viruses adversely affect the general RNA binding properties of the NC domain, and the substantial decrease in viral genomic RNA incorporation observed with some of these mutants is likely to result from the reduced RNA binding properties of NC (11, 12, 27, 45).

Molecular genetic analysis has revealed that RNA sequences essential for packaging of the viral genomic RNA (Ψ) occur near the 5′ end of the unspliced viral genome (5, 46). There are additional regions of the genome that facilitate encapsidation in the presence of Ψ, and these are located proximal to the major subgenomic splice donor and at the 5′ end of the Gag-coding sequence (5, 35, 36, 46). The prevalent species present in wild-type viral particles is the viral genomic RNA, with a 10-fold preference for the viral genomic RNA over the spliced viral RNA in HIV-1 (44). In some NC mutants the ability to preferentially package viral genomic RNA is reduced although the total amount of viral RNA incorporated in the particle is not (44). Alteration of NC can cause loss of packaging of genomic RNA and increased packaging of spliced viral RNA

* Corresponding author. Mailing address: Department of Medicine, Children's Hospital, and Department of Pediatrics, Harvard Medical School, 300 Longwood Ave., Boston, MA 02115. Phone: (617) 355-8426. Fax: (617) 566-4721. E-mail: anna.aldovini@tch.harvard.edu.

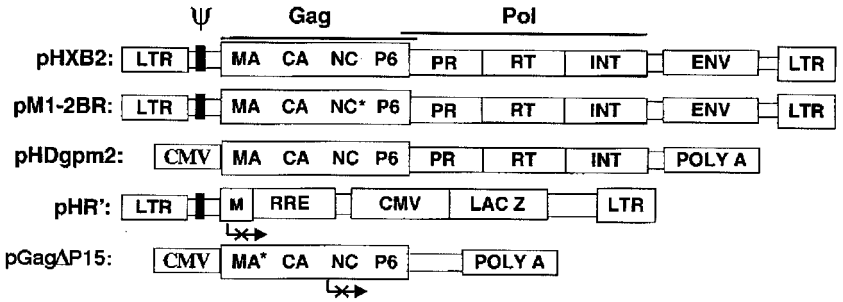

FIG. 1. Schematic representation of the constructs. pHXB2gpt and the pM1-2/BR mutant are, respectively, a wild-type HIV provirus and an HIV provirus with 10 mutations in NC (34, 45). pHDgpm2 expresses HIV Gag and Gag-Pol polyproteins from a sequence whose codons were optimized according to the human codon usage. Although encoding the same protein, this *gag* sequence is 24% different from the original viral sequence. pHDgpm2 does not contain an HIV-1 packaging sequence, and *gag* gene expression is driven by the CMV promoter. pHR′ contains the HIV-1 *cis*-acting sequences necessary for packaging (41). pGagΔ15 expresses an HIV-1 Gag truncated product (stop codon at the end of p2) in a Rev-independent fashion (31). LTR, long terminal repeat.

and cellular mRNAs (6, 16, 17, 37–39, 44, 54), while alterations of the basic residues affect the general ability to bind RNA (12, 45, 50). In the absence of an RNA containing the viral Ψ sequence (Ψ RNA), cellular RNAs become incorporated in virus-like particles (VLPs), and transcripts for housekeeping genes and tRNAs can be detected among these RNAs (40).

A significant amount of in vivo and in vitro data support a crucial role of RNA molecules in virus morphogenesis (10, 20, 40). Muriaux et al. reported that RNase treatment of viral core preparations disrupts the cores almost entirely and that in the absence of an mRNA species with a specific packaging sequence, cellular RNAs are incorporated in the virion (40). Ganser et al. indicated that in vitro assembly of HIV-1 CA and NC into core structures with the correct conical shape was achieved under physiological conditions only in the presence of RNA molecules, whether the RNA was viral or not. Cones could also form in the absence of RNA but only under very-high-ionic-strength conditions (20). In addition, Schmalzbauer et al. reported that the presence of RNA facilitates Gag precursor cleavage in vitro (50). Although these results argue for a role of RNA molecules in virus morphogenesis, it remains unclear whether RNA is necessary for the assembly of the viral particle or for its continued stability.

Here we show that in the absence of RNA incorporation, Gag assembly at the cell membrane can occur efficiently, but only a fraction of the Gag proteins found in the supernatant can be sedimented as particles. Mutations in the basic amino acids of NC that decrease Gag RNA binding may lead to a significant reduction of particles of the appropriate density, not because these amino acid residues are crucial in protein-protein interactions during assembly at the cell membrane but because they are critical to RNA binding, which in turn is critical to events in the virus life cycle that occur after cell membrane assembly, such as budding or particle stability.

MATERIALS AND METHODS

Plasmid constructs. The constructs used in the experiments described in this report are schematically represented in Fig. 1. The parental viral DNA clone used in these studies is the biologically active plasmid pHXB2gpt, which produces a laboratory-adapted strain of HIV-1 (18). In pM1-2/BR, which was previously described, 10 positively charged residues present in the NC fragment that contains the two zinc binding motifs of NC were changed to alanines (45). In pCMV5 GagΔ15 (abbreviated in this report to pGagΔ15), which was previously described, the portion of the *gag* gene that encodes NC, p1, and p6 was deleted, and therefore the Gag polyprotein is approximately 40 kDa (32). Although the *pol* gene is present in this clone, the deletion of the sequences critical for frameshifting prevents *pol* gene expression. pHR′ is an HIV-based packaging vector that does not encode HIV-1 proteins but contains the HIV-1 *cis*-acting sequences necessary for packaging (41). Nearly 350 bp of the 5′ sequence of *gag* as well as *env* sequences encompassing the Rev response element are included in the pHR′ vector, and a stop codon is introduced at the beginning of the residual MA sequence. pHDgpm2 was obtained from the Harvard Gene Therapy Initiative. pHDgpm2 expresses HIV-1 Gag and Gag-Pol polyproteins from a sequence whose codons were optimized according to human codon usage. Although encoding wild-type Gag and Pol proteins, this *gag* sequence is different from the original viral sequence in approximately 24% of its nucleotides. pHDgpm2 does not contain an HIV-1 packaging sequence, and *gag* gene expression is driven by the cytomegalovirus (CMV) promoter. A plasmid expressing HIV-1 Tat, pCV1 (3), and a plasmid expressing HIV-1 Rev, pcRev (34), were cotransfected with pHDgmp2 and pHR′ to achieve gene expression from the HIV-1 long terminal repeat of pHR′.

Cell lines, transfections, and assays. Transfection in 293T cells was carried out by the calcium phosphate method, using 20 μg of DNA in a 100-mm-diameter petri dish. When the two plasmids pHXB2 and pM1-2/BR were cotransfected at different ratios, the total amount of DNA in the transfection was 40 μg. Cells were maintained in high-glucose Dulbecco modified Eagle medium supplemented with 10% fetal bovine serum and in some experiments were switched to serum- and protein-free medium (Cellgro-Free; Cellgro) after transfection. Transfection efficiency was evaluated by fixing the cells on the plate with 1:1 methanol-acetone for 30 min at −20°C, followed by incubation with an HIV-1-positive human serum (1:250 dilution). Antigen binding by this human serum was detected with a horseradish peroxidase-conjugated secondary antibody. Electron microscopy (EM) was carried out at Advanced Biotechnologies Inc. on sections of embedded particles according to standard procedures. For protein analysis, 293T cells transfected with each mutant were lysed in Laemmli buffer (5% glycerol, 1% sodium dodecyl sulfate, 31.875 mM Tris [pH 6.8], 0.005% bromophenol blue) (31). Quantitative reverse transcriptase PCR (RT-PCR) assay was carried out on cellular RNA extracted from 293T cells and DNase treated to eliminate contaminating DNA according to a previously described procedure (45). Supernatants cleared by low-speed centrifugation and filtered though a 0.45-μm-pore-size Millipore filter were utilized for sucrose gradient or sucrose cushion centrifugation according to previously described protocols (2, 11, 14). Viral pellets were resuspended in 0.1% Triton X-100 for p24 enzyme-linked immunosorbent assay (ELISA) (p24 core profile kit; DuPont). p24 ELISA and RT assay were carried out according to previously published procedures (2). The proteinase K protection assay was conducted by incubation of supernatant aliquots with 10 μg of protease K per ml (24). The reaction was stopped by adding a protease inhibitor cocktail (catalog no. P8340; Sigma), followed by inactivation at 65°C for 10 min and storage at −80°C before the analysis. For Western blot analysis, cellular or viral samples containing equal amounts of p24 were subjected to sodium dodecyl sulfate-polyacrylamide gel electrophoresis, transferred to nitrocellulose, and probed with HIV-1-positive human serum as described previously (45). Protein labeling of cellular and viral proteins was carried out with [^{35}S]methionine and [^{35}S]cysteine for 45 min, and chasing was with unla-

beled medium for 1, 3, and 6 h, as previously described (2, 11, 14). Viral proteins in cell and viral lysates were immunoprecipitated using HIV-1-positive serum and protein-G agarose.

Isopycnic sucrose gradient analysis. Clarified supernatants (500 μl) were directly layered on top of the 10 to 60% discontinuous sucrose gradients and were centrifuged in an SW41 rotor at 80,000 × *g* for 24 h at 4°C (11, 14). Eighteen fractions of 500 μl each were collected from top to bottom. The Gag content in each fraction was assayed by p24 ELISA, and the peak fraction(s) was collected for protein analysis.

Cellular fractionation and floatation assay. 293T cells were cultured in medium containing the HIV-1 protease inhibitor Ritonavir (a gift from S. K. Burchett; Children's Hospital) at the final concentration of 10 μM, during and after transfection (29, 42). Cell lysates were harvested at 30 h posttransfection. For cellular fractionation, transfected cells were lysed in hypotonic buffer (20 mM Tris-HCl [pH 7.8], 10 mM KCl, 1 mM EDTA, 0.1% 2-mercaptoethanol, and protease inhibitors) in the presence or absence of nonionic detergent (1% Triton X-100). The nuclei and unbroken cells were separated by low-speed centrifugation. The membrane-associated and cytosol proteins recovered in the supernatant after this centrifugation were further separated by ultracentrifugation at 100,000 × *g* to produce a membrane pellet (P100) and cytosol supernatant (S100). The P100 fraction was resuspended in the original buffer volume. For Optiprep gradient fractionation, the protocol described by Lindwasser and Resh (32) was carried out with the following modification. Ritonavir (10 μM) and the protease inhibitor cocktail (Sigma) were present in all of the working reagents and buffers during the preparation of the cell lysates. After centrifugation at 170,000 × *g* at 4°C for 4 h, eight 500-μl fractions were collected and analyzed by ELISA and Western blotting.

RT-PCR of particle-associated RNA. After clarification and evaluation of p24 in the media of all of the transfectants, supernatants corresponding to an equal amount of p24 were centrifuged to pellet the virions. Viral RNA was extracted and quantitative RT-PCR was performed according to a previously described procedure (44, 45). RNA samples were obtained from three independent transfections of each construct. RNA samples were reverse transcribed and were subjected to an 18-cycle PCR. The primers used in the RT-PCR were Gag primers specific for HIV MA (HIV910, 5′-CTAGAACGATTCGCAGTTAATCC-3′; HIV1110C, 5′-CTCTTCCTCTATCTTGTCTAAA-3′), Gag primers specific for the HDgpm2 MA sequence (HDgp1438, 5′-CTGGAGCGCTTCGCCGTGAACCC-3′; HDgp1638C, 5′-CTCCTCCTCGATCTTGTCCAGG-3′); and human β-actin-specific primers (5′-ATGTTTGAGACCTTCAACAC-3′; 5′-CACGTCACACTTCATGATGG-3′). Aliquots of particle-derived RNA samples equivalent to 400 ng of p24 were used in RT-PCR carried out with human β-actin primers. This PCR was carried out for 30 cycles. The negative controls included a sample from an RT-PCR lacking input RNA and an RT-PCR with RNA extracted from a mock-transfected supernatant. A PCR with an equivalent amount of RNA that did not undergo reverse transcription was carried out for each sample to exclude incomplete DNase I treatment.

RNA quantification in viral particles. Quantification of DNA-free viral RNA samples extracted from viral particles was carried out according to the procedure described by Muriaux et al. with some modifications (40). Briefly, viral particles present in clarified transfection supernatants were concentrated with a Centriprep YM-30 concentrator (Amicon) and purified through a sucrose step gradient (30). Amounts of viral particles equivalent to 4 μg of p24 were used for the RNA purification, and linear acrylamide at final concentration of 0.02% (Ambion) was added to the samples to facilitate the efficient recovery of the RNA. RNA samples were treated with 1U of RNase-free DNase RQ1 (Promega) per μl for 1 h at 37°C. The assay was validated by using aliquots of diluted RNA amounts in the range between 10 to 100 ng. The absence of DNA contamination was confirmed by PCR using HIV-1 MA-specific primers and [^{32}P]dCTP in a 30-cycle reaction. A Ribogreen quantification kit (Molecular Probes) was used to quantitate the RNA according to the procedure suggested by the manufacturer, with some minor modifications. Sequentially diluted RNA samples were mixed with an equal volume of the Ribogreen reagent in a final volume of 200 μl in 96-well plate (Strip Plat-8; Costar). Quantification was carried out using the low range rRNA standards that provide a linear readout at the RNA concentrations of the experimental samples. The emission of incorporated Ribogreen was measured at 535 nm with excitation set at 485 nm on an HTS7000plus Reader (Perkin-Elmer).

RESULTS

Particle production of M1-2/BR, a mutant virus that shows reduced RNA incorporation. Seventeen of the 55 amino acid residues in HIV-1 NC p7 are basic. Cimarelli et al. reported that replacement of positively charged residues with alanines affects particle assembly (11). A number of experimental observations suggested to us that cell membrane assembly of the Gag polyprotein with mutations affecting the basic NC residues was unlikely to be altered significantly and that postassembly defects were a more biologically plausible explanation for the phenotype of these mutants.

TABLE 1. Analyses of p24 and RT in culture supernatants[a]

Construct	p24 (ng/ml)		RT (counts/ml, 10^8)	
	Supernatant	Pellet	Supernatant	Pellet
pHXB2	2,238 ± 186	1,833 ± 43	6.3 ± 0.2	5.9 ± 0.4
pM1-2/BR	2,128 ± 248	178 ± 6	3.9 ± 0.3	0.4 ± 0.1
pGagΔ15	5 ± 4	1 ± 1	ND[b]	ND

[a] Amounts of p24 and RT in the clarified supernatants and in the pellets after centrifugation through a 20% sucrose cushion were estimated. Means ± standard errors were derived from three independent transfections, and each supernatant was evaluated in duplicate.
[b] ND, not done.

We evaluated the amount of Gag protein released into the supernatant from the transfection of pHXB2 (a wild-type clone of HIV-1), pM1-2/BR, and pGagΔ15. In the M1-2/BR mutant virus, 10 of the 17 positively charged residues were changed to alanines, and incorporation of genomic and spliced mRNAs was essentially abolished (45). In pGagΔ15, the NC and p6 proteins are deleted. Mutants with a similar deletion were shown to be deficient in particle assembly and release (23, 26, 28, 33). The amount of Gag-associated p24 as evaluated by ELISA and the RT activity measured in the clarified supernatants and in the viral particles sedimented through a sucrose cushion are reported in Table 1. Cells transfected with pHXB2, pM1-2/BR, and pGagΔ15 showed similar transfection efficiencies and similar accumulations of intracellular viral protein (Fig. 2). Cells transfected with pHXB2 and pM1-2/BR released comparable levels of Gag, suggesting similar levels of particle release (Table 1). The RT activity measured for M1-2/BR was approximately 70% of the activity detected for HXB2. How-

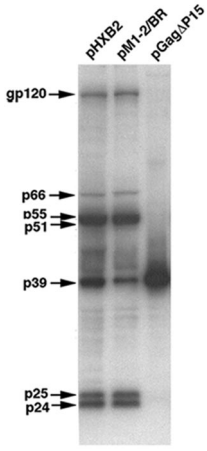

FIG. 2. Analysis of intracellular viral protein accumulation. Equal amounts of pHXB2, pM1-2/BR, and pGagΔ15 cell protein lysates were analyzed by Western blotting, using an HIV-positive human antiserum. The Gag precursor in the pGagΔ15 mutant is approximately 40 kDa because the NC, p1, and p6 domains are deleted.

ever, supernatants from cells transfected with pGagΔ15 contained less than 1% of Gag-associated proteins relative to that found in supernatants derived from cells transfected with pHXB2 and pM1-2/BR. When the amount of Gag in the pellet was evaluated after supernatant centrifugation, only about 10% of the Gag protein detectable in the pM1-2/BR supernatant could be recovered in the sedimented particles. This recovery was approximately 80% for the pHXB2 clone. These results suggested that particle release is highly impaired in pGagΔ15 and that a large fraction of Gag products released from the M1-2/BR mutant were no longer particle associated at the time of centrifugation.

To analyze the morphology of the particles produced by pM1-2/BR and pHXB2, EM was carried out on transfected 293T cells. M1-2/BR particles were easily observed budding from cells in the extracellular space; indeed, they were detected as frequently as wild-type virus (Fig. 3). They were distinct from cellular projections by the presence of a thickened membrane and surface decoration. Although EM does not provide a quantitative assay, significant quantitative differences can be appreciated during scanning. Thus, if M1-2/BR particle production was reduced 10-fold, one would expect the number of mutant particles detected in multiple EM fields to be substantially reduced relative to that for the wild type, but this was not the case. All of the mutant particles showed a typical immature morphology and a slightly larger size than that typical of the mature particle. No mature capsid cores were observed in any of the particles, although some particles contained amorphous matrix having moderate electron density (data not shown).

To more thoroughly characterize the phenotype of the pM1-2/BR mutant, and in particular the sedimentation characteristics of viral proteins released by the mutant in culture supernatant, isopycnic centrifugation of transfection supernatants was carried out (Fig. 4A). Two major peaks of Gag-associated p24 were observed in the gradient fractions. Peak 2 (p2) contained typical retroviral particles, as the density of the fraction corresponding to this peak falls into the normal range for the density of retroviral particles (1.15 to 1.17 g/ml). Peak 1 (p1) corresponded to low-density fractions, which most likely contained monomeric and oligomeric Gag polyproteins. For the wild-type virus, the amounts of Gag-associated p24 present in p1 and p2 fractions were approximately 20 and 80%, respectively, of the total Gag-associated p24 present in the HXB2 supernatant. The values for p1 and p2 were approximately 90 and 10%, respectively, for M1-2/BR. As expected, freeze-thaw cycles, which disrupt viral particles, shifted the amounts of Gag-associated p24 from p2 to p1 in the gradients with wild-type virus (data not shown). The amount of Gag-associated p24 present in the p2 fractions of the two constructs, and measured in our experiments, was consistent with the observations of Cimarelli et al. on viral particles after centrifugation through a sucrose cushion (11). Those investigators focused their analysis exclusively on sedimented virions; analysis of non-pellet-associated viral proteins present in the supernatant was not reported. We were therefore interested in further investigation of the viral proteins present in the low-density fraction of the gradient, where most of the mutant Gag protein was present.

For both wild-type and mutant viruses, Western blot analysis revealed that the viral protein contents of the p1 and p2 fractions were similar (Fig. 4C). As a control, the levels of accumulated intracellular viral protein and the proteolytic processing pattern of HXB2 and M1-2/BR were determined and are shown in Fig. 4B. These results, and additional considerations, suggest that the proteins in the p1 and p2 fractions may be derived from particles. Considering that Gag has a myristoylation signal that targets it to the cell membrane but does not have a secretion signal, it is unlikely that viral proteins present in the p1 fractions were derived from Gag molecules directly secreted from the cell in the absence of particle assembly and release. If this were the case, viral proteins should also be found in the pGagΔ15 supernatant. Similar levels of cell death were observed in the transfections of the three viral clones. In addition, their supernatants were clarified by low-speed centrifugation and by filtering through a 0.45-μm-pore-size Millipore filter, significantly reducing the possibility that cell-associated material was loaded on the gradient. Therefore, we can exclude the possibility that these proteins were the result of cell lysis, as the levels of these proteins are similar in the pHXB2, pM1-2/BR, and pGagΔ15 supernatants. Taken together, these results raise the possibility that M1-2/BR particles might be assembled at a rate similar to that for wild-type particles and that budding defects or particle instability after release could account for the concomitant occurrence of normal amounts of extracellular Gag and poor recovery of particles with the appropriate density.

Intracellular distribution of mutated Gag complexes. To exclude the possibility that the mutations in NC had an effect on the assembly process, we studied the association of Gag molecules of the wild-type pHXB2 and of the mutants pM1-2/BR and pGagΔ15 with the cell membrane in 293T cells (Fig. 5). The amounts of Gag protein found in the cytosol-derived S100 fraction after hypotonic lysis were similar for the wild type and pM1-2/BR (approximately 20%), but this amount was twice as much for pGagΔ15 (40%) (Fig. 5, upper panel, lanes 2, 5, and 8). A higher percentage of Gag was present in the P100 fractions of pHXB2 and pM1-2/BR (~80%), while this percentage was around 60% for pGagΔ15 (Fig. 5, upper panel, lanes 3, 6, and 9). These fractions showed similar profiles for the wild type and mutant constructs when cell lysis was carried out in the presence of a nonionic detergent (Fig. 5B, lower panel). Similar results were observed with Cos-1 cells (data not shown). These results indicate that a higher percentage of pM1-2/BR Gag than of pGagΔ15 Gag is membrane associated.

We also evaluated whether the mutated M1-2/BR Gag molecules associate with fractions of the cell membrane that are defined as barges or with rafts. Barges are membrane microdomains that have a higher density than standard rafts, probably due to the presence of the oligomeric Gag complexes, which localize at these regions during virus assembly (32). When assembly is impaired, as is the case with NC deletions, most of Gag is found associated with standard raft fractions and not at the density of the barge complexes (32).

We carried out a floatation experiment to determine which fraction of M1-2/BR Gag molecules targeted to the cell membrane associated with barges (Fig. 6). As our viruses carry the gene for an active protease, and intracellular Gag processing makes it difficult to estimate the total amount of Gag correctly targeted to the cell membrane, we carried out transfections in

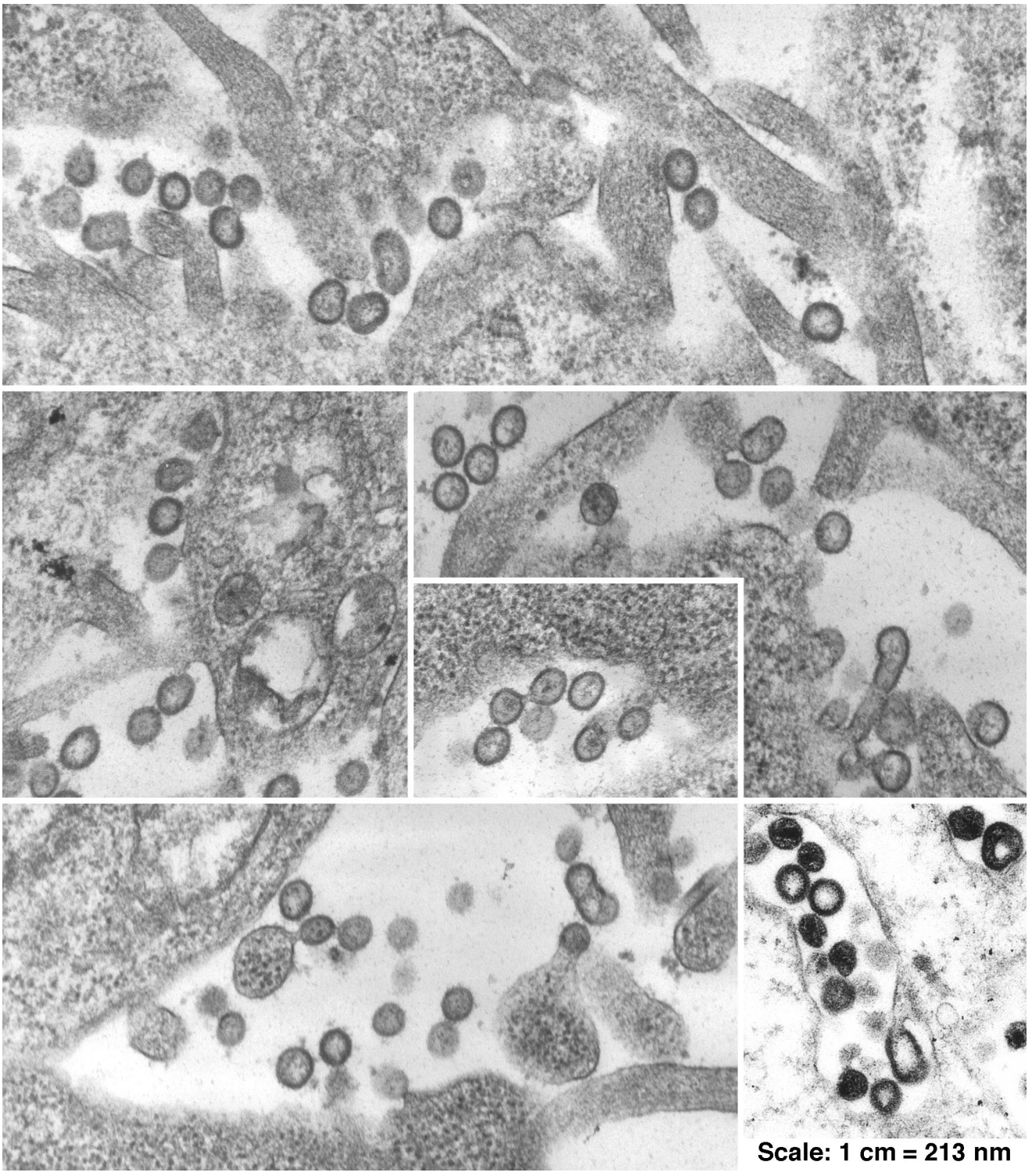

FIG. 3. EM of M1-2/BR viral particles. The panels show particles from multiple fields of pM1-2/BR-transfected cells. The last panel at the bottom on the right shows wild-type HIV-1 from pHXB2. Magnification, ×47,000.

the presence of 10 μM Ritonavir, an inhibitor of the HIV-1 protease. When the total cell lysates derived from these transfections were analyzed by Western blotting, Gag processing was found to be inhibited almost completely by this concentration of HIV-1 protease inhibitor (Fig. 6A). Western blot analysis of samples from fractions recovered from the Optiprep density gradient showed that the fraction richest in Gag molecules was fraction 5, both for wild-type virus and for M1-2/BR (Fig. 6B). This fraction contains the barge membrane microdomains (32). In addition, the distributions of the

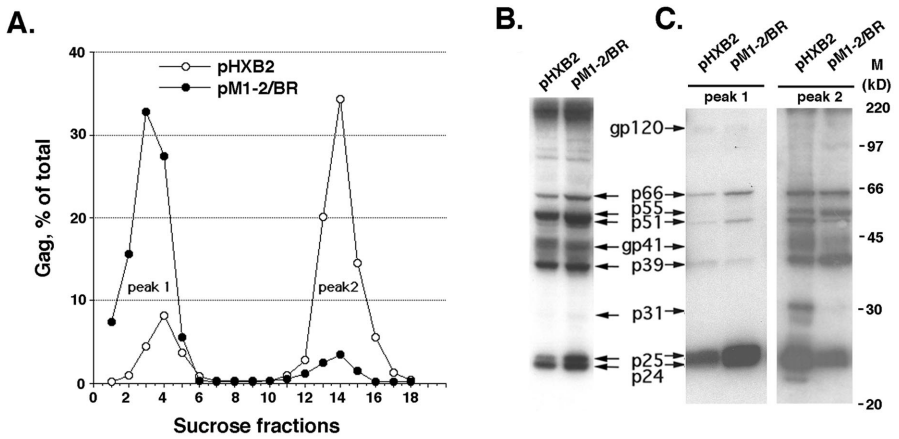

FIG. 4. Sucrose gradient and Western blot analyses of HXB2 and M1-2/BR viral particles. (A) Sucrose gradient fractionation of extracellular Gag. Gag protein amounts in each fraction were measured by p24 ELISA and expressed as percentage of the total p24-assocated Gag harvested from the gradient. The densities (in grams per milliliter) of p1 and p2 were 1.03 ± 0.03 and 1.61 ± 0.01 for HXB2 and 1.03 ± 0.01 and 1.15 ± 0.02 for M1-2/BR, respectively. (B) Western blots of pHXB2 and pM1-2/BR cell lysates. HIV-1 proteins were detected with an HIV-positive human serum. (C) Protein profiles of HXB2 and M1-2/BR sucrose fractions corresponding to p1 and p2. M, markers.

residual Gag were very similar for the two viruses, with minimal amounts of Gag associated with the more typical raft fractions (fractions 2, 3, and 4) (32). Our data indicate that the positive charge present in NC is not necessary for the protein-protein interactions occurring at the cell membrane in which NC is involved and that are critical to virus assembly. The experiments presented so far are inconsistent with the possibility that the lower recovery of sedimented particles in the supernatant of M1-2/BR was due to an assembly defect, as has been suggested previously (11). Although we cannot exclude the possibility of defects in the assembly and budding occurring after cell membrane Gag complex formation, as they are beyond the limits of this assay, the results presented in Fig. 5 and 6 led us to consider more seriously the possibility that the defect exhibited by M1-2/BR virus might be due to particle instability.

Mutations in charged residues of NC molecules and particle stability. To evaluate how wild-type and mutant particle accumulation is affected by time in cell supernatants, we analyzed the protease K sensitivity of particles accumulated in the supernatant for increasing increments of time. Viral proteins contained within the viral particle are resistant to protease K because they are protected by the cell membrane, while monomeric or oligomeric Gag that is not particle associated is protease K sensitive (24). We treated the particles that had accumulated in the supernatants for progressively longer periods of time (1, 5, 9, and 13 h) with protease K and determined the percentage of the total Gag present in the supernatant that was protease K resistant (Table 2). As expected, greater amounts of Gag proteins were detected after longer time intervals, suggesting the continuous accumulation of virus-associated proteins. Approximately 20% of the Gag proteins from HXB2 were protease K sensitive in all supernatants. In contrast, approximately 80% of the Gag proteins from M1-2/BR were protease K sensitive. The percentage of protease K-sensitive Gag was independent of the total amount of accumulated Gag, and the percentage was the same whether virus production had occurred for 1 h or for 13 h. Similar results were observed when we carried out a pulse-chase experiment. As the length of the chase increased, larger amounts of pelleted particles were detected for both HXB2 and M1-2/BR. However, the amounts were consistently lower for M1-2/BR than for HXB2 at each time point that we analyzed (data not shown). The experiments described thus far suggest that the Gag molecules detected in the supernatant of M1-2/BR could be derived from released viral particles that are unstable and that their disruption may occur rapidly, most likely in less than an hour, after release.

To further evaluate the effects of the NC mutations on particle production, we produced mosaic virions containing different ratios of wild-type HXB2 and M1-2/BR mutant Gag, allowing us to evaluate the influence of mutant Gag in the context of wild-type, assembly-competent protein (Fig. 7). If

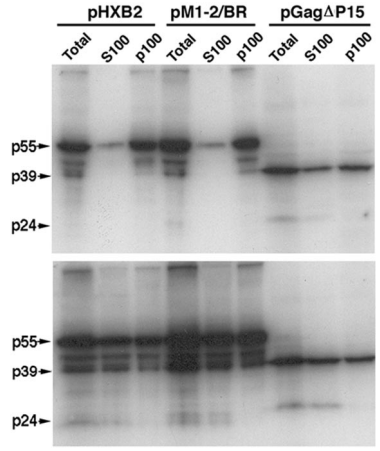

FIG. 5. Cellular fractionation of transfected-cell lysates. The S100 and P100 fractions were obtained after ultracentrifugation of the clarified cell lysates. (A) Transfected cells from the individual transfection were lysed in hypotonic buffer in the absence of detergent. (B) Transfected cells were lysed in hypotonic buffer in the presence of Triton X-100.

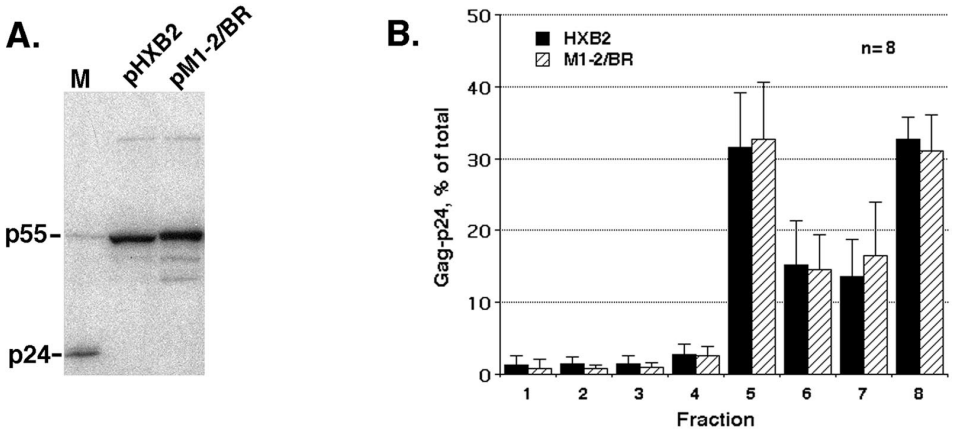

FIG. 6. Gradient fractionation of intracellular HXB2 and M1-2/BR Gag. (A) Western blotting of total HXB2 and M1-2/BR cell lysates. Lane M, markers. The presence of Gag-related bands smaller than Pr55 could be due to less-than-optimal inhibition of the HIV protease and/or internal initiation at the capsid Met142 (8). (B) Floatation of Triton X-100-extracted cell protein lysates in an eight-fraction Optiprep gradient. The histogram illustrates the results derived from the Western blot and ELISA analyses of the fractions of eight independent gradients. Error bars indicate standard deviations.

the NC mutations affect particle stability, one would expect that an increase in the ratio of mutant to wild-type Gag in mosaic particles would lead to a decrease in particle stability. We carried out the cotransfections under six different conditions, where the total amount of DNA was held constant and the ratios of pHXB2 to pM1-2/BR were varied in each transfection (lanes a, 5:0; lanes b, 4:1; lanes c, 3:2; lanes d, 2:3; lanes e 1:4; lanes f, 0:5). Since the flotation experiment described above did not reveal a cell membrane assembly defect for M1-2/BR, we assumed that the ratio of wild-type and mutated Gag molecules incorporated into particles would reflect the intracellular ratio of the two species, and this was confirmed experimentally (see below). Increasing amounts of M1-2/BR did not result in any anomaly in Gag accumulation and processing in cells, as judged by Western blot analysis of cell lysates (Fig. 7A). The total amounts of accumulated Gag were similar in all transfection supernatants (data not shown). As an indication that the M1-2/BR Gag became incorporated into the mosaic particles at increasing levels, a higher percentage of unprocessed Gag could be detected as the ratio of M1-2/BR DNA used in the transfection increased (Fig. 7B, lanes 2 to 5). This reduced rate of Gag processing is a feature of M1-2/BR Gag particles (Fig. 4C, peak 2) (45). To determine the relative level of stable particles produced in each transfection, we examined the effect of protease K treatment on the mosaic particles containing different ratios of wild-type and mutant Gag (Fig. 7 B and C). Despite the larger amounts of M1-2/BR Gag, the majority of Gag present in the supernatants was associated with protease-resistant particles. Since the increase in the ratio of mutant to wild-type Gag in mosaic particles did not produce a substantial decrease in the amount of pelleted particles, it is unlikely that the NC mutations per se affected particle production.

We entertained the possibility that the incorporation of RNA, facilitated in mosaic particles by wild-type Gag, favors post-cell membrane assembly events or particle stability. To determine the extent to which the presence of HXB2 Gag molecules in the mosaic particles influenced viral RNA incorporation, we measured the incorporation of viral genomic RNA in the particles derived from the six different transfection conditions (Fig. 7D). Viral genomic RNA incorporation varied between 100 and 80% in the particles pelleted from supernatants a, b, c, and d and was approximately 65% in the particles derived from supernatant e. Very little viral genomic RNA could be detected in particles derived from supernatant f, as shown previously (45). Thus, significant increases in the ratio of mutant to wild-type Gag in the mosaic particles did not result in a commensurate decrease in RNA incorporation. We conclude that the presence of HXB2 Gag facilitated the incorporation of RNA in these mosaic particles and that the amount of viral RNA present in these particles is a better predictor of the amounts of particles that can be sedimented than the amount of mutant Gag, suggesting a role for RNA in particle stability.

There is evidence that nonviral RNA or DNA molecules can be incorporated into viral particles (9, 10, 40). We have previously shown that M1-2/BR does not incorporate significant amounts of genomic or spliced viral RNA (45), and others have shown that mutations of positively charged residues decrease nonspecific RNA binding by NC (11, 50). It is possible

TABLE 2. Recovery of protease K-resistant p24 in culture supernatants[a]

Virus production (h)	p24 (ng/ml)		Protease K-resistant p24 (%)	
	HXB2	M1-2/BR	HXB2	M1-2/BR
1	55 ± 5	103 ± 11	79 ± 6	12 ± 2
5	263 ± 17	636 ± 46	90 ± 5	10 ± 2
9	544 ± 51	1,149 ± 154	90 ± 5	7 ± 2
13	1,057 ± 239	1,315 ± 160	75 ± 6	12 ± 2

[a] Amounts of p24 in the protease K-treated and nontreated supernatants were estimated by ELISA. The recovery of p24 is defined as the amount of p24, reported as percentage of the untreated supernatant, that could be measured in the supernatant after the protease K treatment. Means ± standard errors derived from two independent experiments in which each sample was evaluated in duplicate are reported.

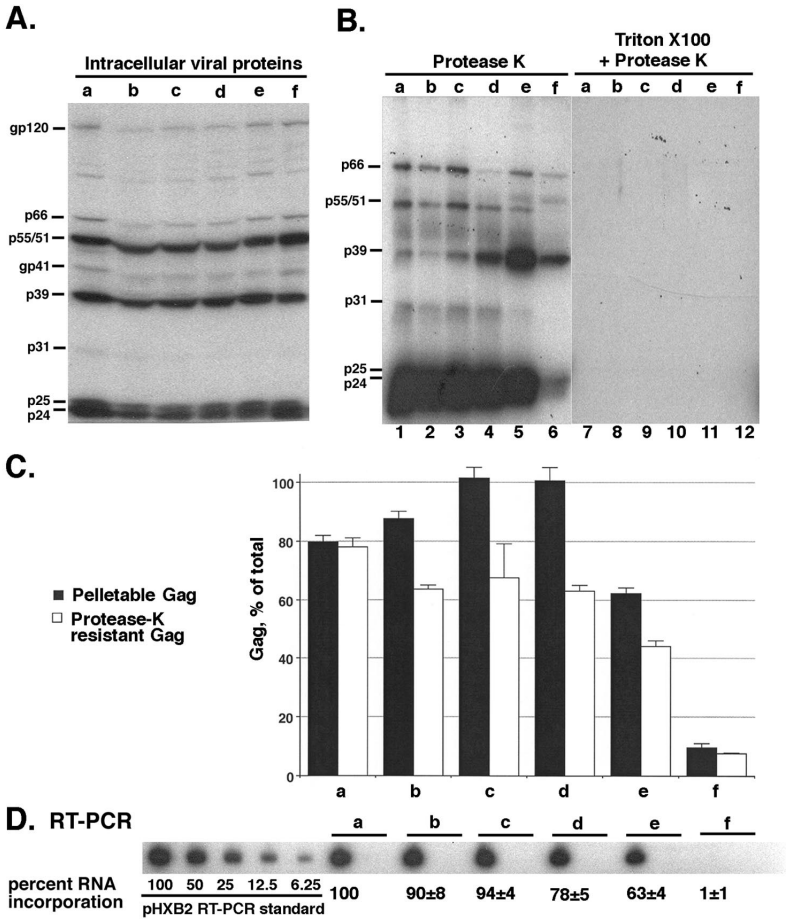

FIG. 7. Analysis of mosaic particles composed of HXB2 and M1-2/BR Gag molecules. In each panel lane a corresponds to a sample derived from the transfection of pHXB2 alone; lanes b, c, d, and e correspond to samples derived from the transfection of pHXB2 and pM1-2/BR at ratios of 4:1, 3:2, 2:3, and 1:4, respectively; and lane f shows the analysis of a sample derived from the transfection of pM1-2/BR alone. (A) Western blot analysis of intracellular viral proteins. (B) Western blot analysis of mosaic viral particles. Particles were pelleted through a 20% sucrose cushion after supernatant clarification. An amount of supernatant corresponding to 100 ng of p24 was used in the Western blotting of protease K-treated samples (lanes 1 to 6) and of Triton X-100- and protease K-treated samples (controls, lanes 7 to 12). (C) Relative stability of mosaic particles. The histogram shows the percentage of pellet-associated Gag and of protease K-resistant Gag present in each supernatant derived from the cotransfection of different amounts of pHXB2 and pM1-2/BR. The percentage of particle-associated Gag was calculated relative to the amount of Gag present in the untreated supernatant before centrifugation. Gag associated with protease K-resistant particles was evaluated directly in the supernatant after protease K treatment. Three independent experiments were carried out and each supernatant was tested in duplicate. Error bars indicate standard errors. (D) RT-PCR analysis of viral genomic RNA incorporation in pelleted viral particles. Standards for viral genomic RNA were derived from twofold dilutions of the HXB2 RNA samples. The results of one representative experiment are shown here (for each sample, the first lane corresponds to an RNA sample that was subjected to RT-PCR and the second corresponds to an RNA samples that was subjected to PCR only). The percentage of RNA incorporation for each sample was evaluated by comparison to the standards in four independent experiments and is reported with its standard error at the bottom.

that the protease K-resistant particles detectable in M1-2/BR supernatants reflect the residual ability of this mutant to bind and incorporate RNA molecules in a nonspecific fashion. The M1-2/BR NC protein retains 7 of the 17 positively charged residues present in the wild-type protein. It remains unclear whether the absence of RNA and the presence of mutations in positive residues of NC both contribute to particle instability or if one of the two factors takes precedence over the other in defining this phenotype. Given the phenotype of the mosaic particles produced in cotransfection e, where M1-2/BR Gag molecules are present in larger amounts than HXB2 Gag molecules (ratio of HXB2 to M1-2/BR, 1:4), we hypothesized that the absence of RNA is more critical than the presence of an intact NC for particle stability. The next set of experiments addresses the individual roles of these two structural components.

Role of NC integrity in particle stability. To distinguish between the roles of RNA incorporation and NC integrity in particle stability after budding, we evaluated the stability of virion particles produced from a construct that expresses wild-type Gag but does not express an mRNA with an HIV packaging signal. We produced VLPs by using the construct pHDgpm2, which expresses HIV-1 Gag-Pol from a codon-optimized sequence. This Gag-Pol sequence was synthesized using oligonucleotides in which the sequence of each codon was selected according to the preferential codon usage found

in humans. The promoter that directs expression of this sequence is the CMV promoter. Therefore, the entire HIV packaging sequence is missing, including the portion that extends into the Gag-coding sequence, as this portion of the Gag sequence is different from that of HIV-1 in pHDgpm2 and therefore is unlikely to fold into the same RNA secondary structure. The particles produced from this vector were analyzed by isopycnic sucrose gradient centrifugation and Western blotting (Fig. 8A and B). In addition, we analyzed the association of Gag complexes with the cell membrane by floatation assay (Fig. 8C).

The pHDgpm2 *gag-pol* gene expressed in 293T cells resulted in the extracellular release of Gag at slightly higher levels than pHXB2 Gag. This difference probably depends on the different activities of the CMV and long terminal repeat promoters. However, the amount of Gag sedimenting at the appropriate density for a retroviral particle was approximately 50% of the total (Fig. 8A). This amount is different than that observed for a wild-type *gag-pol* gene expressed in a cell that also expresses an RNA containing the entire HIV-1 packaging site (Ψ RNA). When pHDgpm2 and pHR′ were cotransfected in the cells, approximately 80% of Gag consistently sedimented at the appropriate density for particles. Cotransfection of pHDgpm2 with pHR′, a construct that expresses a Ψ RNA, resulted in a larger amount of extracellular Gag being particle associated (Fig. 8A), and this amount was similar to that observed for the virus produced by pHXB2 (Fig. 4A). Intracellular viral protein accumulation was similar in protein lysates from the transfection of pHDgpm2 and pHDgpm2+pHR′ (Fig. 8B). These profiles are comparable to those for the transfection of these cells with pHXB2 (Fig. 4B). When the pHDgpm2 cellular lysate was analyzed in a floatation assay, the distribution of Gag complexes was similar to that for the wild-type virus (Fig. 8C and 6B). These data exclude the possibility that the small reduction in levels of sedimented particles seen with pHDgpm2 compared to pHXB2 is due to less efficient assembly at the cell membrane.

Taken together, the experimental data described thus far suggest that the presence of an intact NC protein in the Gag molecule is insufficient to obtain wild-type levels of particles after sedimentation in the absence of a Ψ RNA and, furthermore, that the level of RNA incorporation into particles may be a critical factor for particle stability.

Role of viral and cellular RNA incorporation in viral particle stability. To evaluate further whether the stability of viral particles correlates with the incorporation of Ψ RNA and cellular RNA, we measured the amount of incorporated Ψ RNA and other mRNAs in sedimented particles (Fig. 9A). Efficient Ψ RNA incorporation was detected in viruses produced by pHXB2 and by pHDgpm2+pHR′ but not in those produced by pM1-2/BR (Fig. 9A, lanes 1, 2, and 4). RT-PCR carried out with primers corresponding to the HDgmp2 sequence produced a faint signal in RNA from virus produced by pHDgpm2 but not in that from virus produced by pHDgpm2+pHR′ (Fig. 9A, lanes 7 and 8). Amplification of the pHDgpm2 *gag* mRNA, which does not contain an HIV Ψ sequence or a wild-type HIV-1 Gag sequence, was selected as a means to detect possible incorporation of cellular messengers. This analysis indicated that pelleted particles released from HDgpm2 incorporated cellular RNA species when a Ψ RNA was not present (Fig. 9A, lane 7). Incorporation of cellular RNA was not favored when a Ψ RNA was present (Fig. 9A, lanes 4 and 8). The band intensity obtained with HDgpm2-specific primers cannot be quantitated, as the intensity of this band cannot be compared to the intensity of the Ψ RNA. Nevertheless, the detection of this RNA is a qualitative indication that mRNAs present in the cytoplasm can become in-

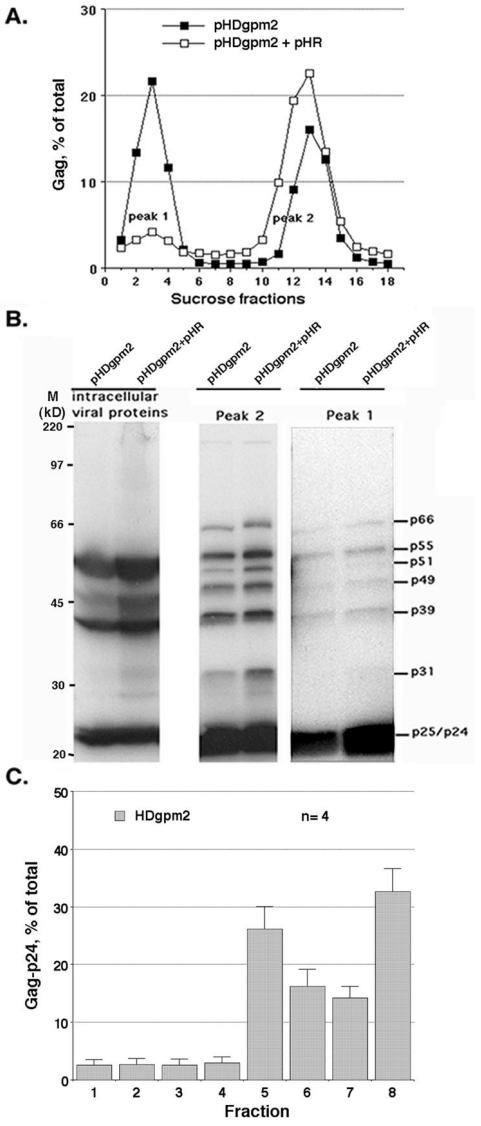

FIG. 8. Gradient analysis of VLPs (pHDgpm2) and VLPs produced in presence of a Ψ RNA (pHDgpm2+pHR′). (A) Gag distribution in sucrose gradient fractions. The densities (in grams per milliliter) of p1 and p2 were 1.03 and 1.16 for the peak fractions of the gradient loaded with particles from the pHDgpm2 transfection and 1.04 and 1.16 for the peak fractions of the gradient loaded with particles from the pHDgpm2+pHR′ transfection, respectively. This analysis was repeated three times with comparable results. (B) Western blots of pHDgpm2 and pHDgpm2+pHR′cellular lysates. Sucrose fraction aliquots corresponding to 80 ng (peak 2) and 40 ng (peak 1) of p24 were analyzed. M, markers. (C) Floatation assay of Triton X-100-extracted pHDgpm2 cell proteins in an eight-fraction Optiprep. The histogram illustrates the results derived from the Western blot and ELISA analyses of the fractions of four independent gradients. Error bars indicate standard deviations.

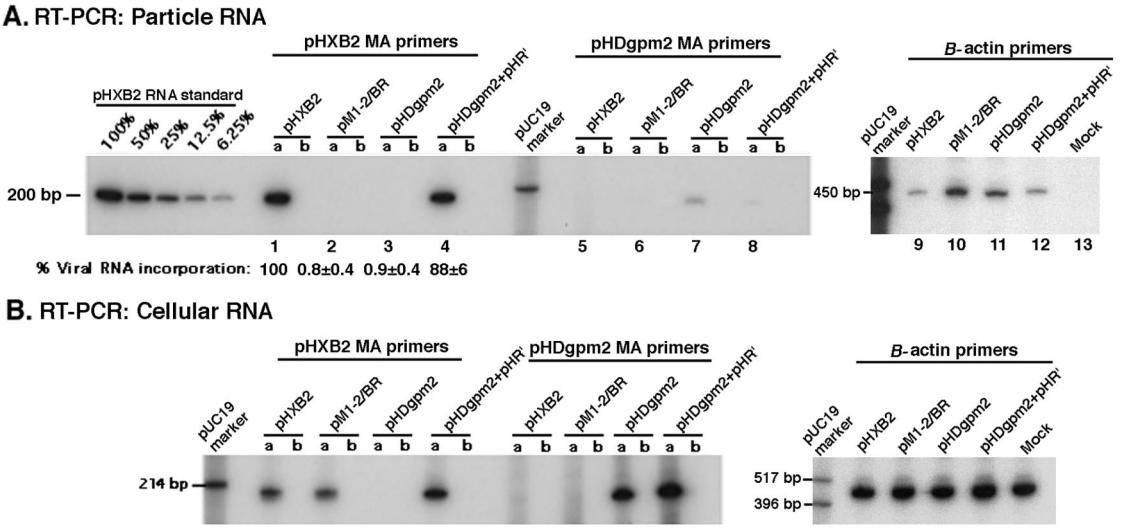

FIG. 9. RNA incorporation in wild-type and mutant viral particles. (A) RT-PCR of particle-derived RNA. The results of one representative experiment are shown. The mean and the standard error of the Ψ RNA content in samples analyzed in duplicate from three independent experiments are reported under lanes 1 to 4 (HIV-1 MA-specific primers). Detection of RNA carried out with pHDgpm2-specific primers (lanes 5 to 8) and with β-actin-specific primers (lanes 9 to 13) is also shown. Lanes a, RNA samples subjected to RT-PCR; lanes b, RNA samples subjected to PCR only. (B) RT-PCR of cellular RNA. Cellular RNA samples equivalent to equal amounts of total RNA were used in RT-PCRs with HIV-1 MA-, HDgpm2-, or actin-specific primers. Transfection efficiencies were comparable for all of the plasmids. Lanes a, RNA samples subjected to RT-PCR; lanes b, RNA samples subjected to PCR only.

corporated into the viral particle in the absence of Ψ RNA. Therefore, it is likely that a variety of cellular mRNAs, in addition to pHDgpm2 Gag-Pol mRNA, were incorporated into these particles.

To further investigate the presence of cellular RNA in particle-derived RNAs from the different viruses, we carried out an RT-PCR using actin-related primers (Fig. 9A, lanes 9 to 13). Our rationale was based on the fact that actin mRNA is very abundant in the cytoplasm and therefore is a likely candidate for nonspecific RNA incorporation. Unlike the RT-PCRs shown in Fig. 9A, lanes 1 to 8, which were carried out for 18 cycles, these reactions were carried out for 30 cycles. Actin was more easily detected in sedimented particles that did not contain a Ψ RNA. In M1-2/BR and HDgpm2 particles, we found amounts of β-actin RNA equivalent to, respectively, seven- and fourfold the amount we found in HXB2, while the amount found in HDgpm2+HR′ was comparable to that in HXB2. These data support the notion that cellular RNA is present in the particles that can be pelleted by centrifugation (Fig. 9A, lanes 10 and 11). Amplification of intracellular *gag* mRNA was carried out to exclude the possibility of significant differences in the amounts of transcribed Gag RNA for the different constructs (Fig. 9B). Measurements of the total amounts of RNA in aliquots of supernatants and pellets containing equal amounts of p24 confirmed that RNA was present in the pelleted M1-2/BR and HDgpm2 virions in amounts similar to those of pelleted HXB2 or pHDgpm2+pHR′, which preferentially incorporated Ψ RNAs (Table 3). There is a direct correlation between the percentage of the amount of RNA present in the supernatant and the amount of pelletable Gag (Table 3). We conclude that the particles recovered in the pellet after centrifugation contain RNA that is packaged specifically or nonspecifically. In the absence of a Ψ RNA, cellular RNAs are incorporated.

The pulse-chase experiment and the experiments reported in Table 2 show that time is not a factor affecting the recovery of M1-2/BR particles, as we do not find a lower level of sedimented particles over time. When considered with the experiment presented in Fig. 9, these data support the conclusion that the amount of protease-resistant Gag (or of stable particles) is determined by the presence of RNA in particles. The percentage of particles incorporating RNA present in the supernatant does not change with time, as it is determined at the time of budding. Therefore, the percentage of protease-resistant Gag also does not change with time and is independent of the level of Gag accumulation. These data confirm that RNA incorporation plays a role in the structural integrity of the viral particle.

The data reported in Fig. 8 and Table 3 also show that the relative amounts of viral proteins found in p2 and p1 can appear to redistribute when two different experiments are

TABLE 3. RNA content of viral supernatants and pelleted particles[a]

Construct	Extracellular Gag		Particle RNA (% of ng of p24)	
	Supernatant (ng/ml)	Pellet (% supernatant)	Supernatant	Pellet
pHXB2	2,574 ± 43	75 ± 4	100	100
pM1-2/BR	2,085 ± 378	7 ± 1	25 ± 5	94 ± 9
pHDgmp2	1,994 ± 204	55 ± 3	64 ± 10	95 ± 8
pHDgmp2 + pHR	2,803 ± 509	88 ± 9	106 ± 17	99 ± 5

[a] All reported percentages and their errors were approximated to the closest integer. RNA in aliquots of the clarified supernatants and of the pelleted virions containing equal amounts of p24 was estimated. A Ribogreen quantification kit (Molecular Probes) was used to quantitate the RNA. Means ± standard errors derived from three independent experiments are reported. The background from mock-transfected cells was consistently lower than 7%.

compared. When wild-type Gag is expressed in the presence of a Ψ RNA, most of the of the viral proteins are in p2 (Fig. 8A, pHDgpm2+pHR). When a smaller amount of cellular RNA is incorporated by the particles produced in absence of a Ψ RNA, more viral proteins are found in p1 (Fig. 8A, pHDgpm2). Under these two different experimental conditions, the amount of Gag in the supernatant does not change (Table 3). Different percentages of Gag are found in p2 or p1 fraction, depending upon the total amount of RNA present in the particles (Table 3).

DISCUSSION

The retroviral NC protein appears to have roles at multiple stages of the virus life cycle. As a domain of the Gag precursor, it is involved in Gag-Gag interactions that are critical to assembly and in RNA binding and packaging (see references 46 and 51 and references therein). The processed NC p7 may be involved in early steps of the infection process (48). In this report, we show that the basic charge present in NC is crucial to NC-RNA interactions but not as crucial to Gag-Gag interactions at the cell membrane. No major defects in membrane association or in the amount of Gag released in the supernatant were observed for the pM1-2/BR mutant. Therefore, it is unlikely that the basic residues present in the two zinc binding motifs mediate the role played by NC in virus assembly. We also show that there is a direct correlation between the percentage of Gag that is associated with RNA and the amount of Gag that can be pelleted as particle associated. Particles that band at the appropriate density for a retrovirus are particles that incorporate RNA. Two possible interpretations can be offered for the origin of the Gag proteins found in the supernatant that are not particle associated. They can derive from RNA-deficient, barge-associated Gag complexes that do not complete the proper assembly and budding process and are released in some manner from the cell. Alternatively, assembly and budding are completed successfully, independently of the presence of RNA in the barge complexes; particles that do not package RNA are highly unstable after release and become quickly disrupted, leading to the accumulation of viral proteins in the supernatant. We favor the latter hypothesis.

The presence of an RNA species, perhaps in dimer form, is critical for achieving correct particle morphology, as the RNA functions as a scaffold in particle assembly and maturation (10, 20). Maturation of the particle is linked to postbudding processing of the viral precursors Gag and Gag-Pol and to the condensation of CA and NC on the RNA. When the particles produced by pM1-2/BR were analyzed by EM, their morphology was that of a PR-deficient virus for virtually all particles. Similar particle morphology and frequency were reported for Gag mutants truncated at the first or second zinc (26, 28). It is difficult to know how many of these newly released particles are among the few that package cellular RNA. It is quite possible that only 10% of these particles have packaged RNA and that the cell pellet EM detects both the particles that will remain intact and those that disassemble in the supernatant, immediately after their cellular release. Lack of an electron-dense core could be due to the absence or incorrect positioning of the RNA and/or to less efficient precursor processing.

We detected comparable amounts of Gag-associated p24 in the supernatants of pHXB2 and pM1-2/BR. We could not detect a similar amount of Gag in the supernatant of pGagΔ15, which is defective in assembly (32). This information, together with the results of cell fractionation and flotation experiments, suggests that M1-2/BR may not have a virus assembly defect. This mutant was proposed to have an assembly defect because the amounts of M1-2/BR pelleted particles observed in pulse-chase experiments were significantly smaller than those for the wild type (11). The relative amounts of pHXB2 and pM1-2/BR Gag-associated p24 that we found in sucrose gradient fractions 13 and 14 (Fig. 4A) are consistent with the results observed by Cimarelli et al., who focused on the analysis of pelleted material (11). They interpreted the significant reduction in M1-2/BR particle recovery after centrifugation to be a consequence of an assembly defect of the mutant. The results described here argue for a different interpretation: that pM1-2/BR may assemble particles, but inefficient packaging of RNA causes particles that are released into the extracellular supernatant to be short lived.

We considered alternative explanations that might account for the observations reported here. It is extremely unlikely that the viral proteins that we detected in low-density fractions are derived from active secretion, from cellular lysis with release of viral proteins, or from cells contaminating the supernatant. The analysis of pGagΔ15 provides a direct control for all of these possibilities. If the M1-2/BR mutant had a significant assembly defect due to reduced Gag-Gag interactions, a higher percentage of Gag would be found in the S100 fraction after hypotonic buffer lysis, as we observed in the case of pGagΔ15. In addition, reduced levels of Gag complexes would have been present in the barge fractions in the flotation experiment. The nonassembled Gag would have been recovered in the lighter raft-like fractions of the cell membrane or in the cytoplasmic material. The profiles of the Optiprep gradient fractions that contain barges were essentially identical for pM1-2/BR and pHXB2 cell lysates and were similar to those reported by others for HIV (32). Therefore, we concluded that this mutant did not have a significant assembly defect, at least within the limits of this assay, and that the soluble viral proteins present in the supernatant of M1-2/BR could derive from disrupted particles.

If M1-2/BR is indeed assembly competent and particles bud from the cell membrane, the results presented in Table 2 show that the disruption of the particles lacking RNA happens very quickly, most likely as soon as the particle moves away from the cell. One interpretation is that these particles without RNA burst in the medium immediately after release. In this case, these particles would not last long enough to band in high-density fractions, and therefore only their protein components can be detected in the low-density fraction. Interestingly, Ganser et al. showed that under physiological conditions, core assembly does not occur in the absence of RNA (20). The salt concentration needs to be at least 1 M in order to obtain assembled CA-NC cores in the absence of RNA. It is possible that particles lacking RNA break down when the protease initiates Gag processing. The Gag-Gag interactions provided by the membrane-bound MA or MA-CA might not be sufficient to retain the appropriate particle structure in the absence of core condensation on the RNA.

We detected a higher accumulation of partially processed

Gag fragments in the M1-2/BR virus than in the wild type, and this was observed in pelleted virions that were found to contain RNA and not intracellularly. It is possible that the Gag protein mutations encoded in M1-2/BR affect the folding of this protein such that the cleavage sites in Gag are less accessible to the viral protease. However, in this case reduced M1-2/BR processing should also be detected within cells, but it was not. Alternatively, the reduced affinity of the mutated M1-2/BR Gag for the incorporated RNA could affect Gag-RNA protein interactions and Gag folding, leading to reduced Gag processing. Interestingly, the M1-2/BR Gag proteins that were found in the low-density fractions of the gradient did not show higher levels of partially processed Gag polyproteins than those of HXB2 (Fig. 4C, peak 1), suggesting that reduced Gag processing occurs only in the pelleted M1-2/BR particles that incorporate RNA.

The analysis of VLPs produced by pHDgpm2 was critical to sort out whether the lack of RNA or the mutations in NC were more critical determinants of the post-cell membrane assembly defects of the M1-2/BR virions. This analysis also confirmed that reduced RNA binding by Gag does not result in reduced assembly at the cell membrane. When a similar analysis was conducted on Moloney murine leukemia virus VLPs, Muriaux et al. concluded that, in absence of a messenger with a virus-specific packaging sequence, 60% of viral particles incorporate cellular RNAs (40). Our data for HIV-based VLPs are in agreement with those reported by Muriaux et al. for Moloney murine leukemia virus. In addition, we have shown that even if only 60% of these particles incorporate RNA and can sediment at the correct density, the amount of Gag present in barge complexes is similar to that observed for the wild-type virions that incorporate higher percentages of RNA. This observation rules out the hypothesis that the Gag molecules that are not bound to RNA interact less favorably with other Gag molecules at the cell membrane and therefore are excluded from these high-density complexes. Muriaux et al. postulated a role of RNA in particle assembly but did not address this question experimentally. The fact that RNA binding is not critical to assembly is also supported by the observation that efficient particle formation and release can still occur when NC is replaced with a non-RNA binding motif, a leucine zipper domain (1, 55). This replacement did not disrupt assembly, as the leucine zipper motif could provide the protein-protein interactions normally provided by NC and necessary for the formation of a multimeric Gag complex. In light of the RNA incorporation data, it is possible that the particles that are present in p2 fractions contain RNA and therefore are stable and do not disassemble into the proteins that band in the p1 fractions. This may occur not just for the wild-type virus but also for our mutant M1-2/BR or the virus with wild-type Gag produced by pHDgpm2, in absence of an RNA with a virus-specific Ψ site. Viral proteins present in p1 fractions may derive from particles that lack RNA and most likely disassemble immediately after release.

Taken together, the data presented in this report suggest that the portion of particles that are found in the supernatant after cellular budding and release correlates well with the percentage of particles that have incorporated an RNA, whether viral or cellular. The amount of RNA packaged reflects the specific and nonspecific affinities of Gag for RNA and its total level depends on whether an RNA with a virus-specific packaging sequence is present in the cytoplasm. In pHDgpm2, the NC protein is not mutated and the affinity of Gag for RNA is intact. As this construct does not encode a Ψ RNA, only nonspecific RNA binding can be achieved by Gag. The lower affinity of Gag for RNA species without a virus-specific packaging signal results in a lower percentage of particles incorporating RNA than when a Ψ-containing RNA species is present. In pM1-2/BR, the significant reduction of positive charge in NC results in a substantial reduction of specific and nonspecific RNA affinities. Therefore, incorporation of viral and cellular RNAs is reduced, and a very limited number of particles that are produced contain RNA. Structural features of the cellular RNAs might be critical in determining the ratios of the different cellular RNAs present in the particles when the NC protein is intact. When NC is mutated and the affinity for RNA is significantly reduced, the relative abundance of a certain messenger in the cytoplasm might be the most significant determinant for its particle incorporation.

The RNA, whether with a virus-specific packaging signal or not, apparently provides the virus with a structural function beyond a simple scaffold. RNA contributes importantly to maintenance of particle integrity, whereas the concept of a scaffold implies a temporary function that can be removed after architectural assembly. The absence of RNA or its removal by RNase treatment leads to particle collapse. Our experiments suggest that RNA incorporation may be more important to stable particle structure than an intact NC protein. At least 50% of Gag in the supernatant in pHDgpm2 was not particle associated, possibly because of loss of stability in the absence of RNA. Particles lacking RNA may disassemble soon after release, whether they consist of Gag molecules that were wild type or have a mutated NC. Furthermore, short-lived particles may account for the low-density viral proteins detected in the sucrose gradients of pM1-2/BR and pHDgpm2 supernatants. Alternatively, it is possible that the absence of bound RNA in the Gag complexes present in the barges leads to aberrant release of these complexes in the supernatant. The reduction of positive charge in NC affects the levels of virus recovery not because this feature of NC is critical to Gag-Gag interactions at the cell membrane, but rather because it is critical to RNA incorporation, which in turn is important for postassembly and budding or particle stability.

ACKNOWLEDGMENTS

This work was supported by NIH grant AI 36060.

We thank John Gray of the Harvard Gene Therapy Initiative and Marilyn Resh of Cornell University for the gifts of the plasmids pHDgpm2 and pCMV5GagΔ15 (abbreviated in this report to pGagΔ15), respectively. In addition, we thank members of our lab and Richard A. Young for critical reading of the manuscript.

REFERENCES

1. **Accola, M. A., B. Strack, and H. G. Gottlinger.** 2000. Efficient particle production by minimal Gag constructs which retain the carboxy-terminal domain of human immunodeficiency virus type 1 capsid-p2 and a late assembly domain. J. Virol. **74:**5395–5402.
2. **Aldovini, A., and R. A. Young.** 1990. Mutations of RNA and protein sequences involved in human immunodeficiency virus type 1 packaging result in production of noninfectious virus. J. Virol. **64:**1920–1926.
3. **Arya, S. K., C. Guo, S. F. Josephs, and F. Wong-Staal.** 1985. Trans-activator gene of human T-lymphotropic virus type III (HTLV-III). Science **229:**69–73.

4. **Bennett, R. P., T. D. Nelle, and J. W. Wills.** 1993. Functional chimeras of the Rous sarcoma virus and human immunodeficiency virus Gag proteins. J. Virol. **67:**6487–6498.
5. **Berkowitz, R., J. Fisher, and S. P. Goff.** 1996. RNA packaging. Curr. Top. Microbiol. Immunol. **214:**177–218.
6. **Berkowitz, R. D., A. Ohagen, S. Hoglund, and S. P. Goff.** 1995. Retroviral nucleocapsid domains mediate the specific recognition of genomic viral RNAs by chimeric Gag polyproteins during RNA packaging in vivo. J. Virol. **69:**6445–6456.
7. **Bowzard, J. B., R. P. Bennett, N. K. Krishna, S. M. Ernst, A. Rein, and J. W. Wills.** 1998. Importance of basic residues in the nucleocapsid sequence for retrovirus Gag assembly and complementation rescue. J. Virol. **72:**9034–9044.
8. **Buck, C. B., X. Shen, M. A. Egan, T. C. Pierson, C. M. Walker, and R. F. Siliciano.** 2001. The human immunodeficiency virus type 1 *gag* gene encodes an internal ribosome entry site. J. Virol. **75:**181–191.
9. **Campbell, S., and A. Rein.** 1999. In vitro assembly properties of human immunodeficiency virus type 1 Gag protein lacking the p6 domain. J. Virol. **73:**2270–2279.
10. **Campbell, S., and V. M. Vogt.** 1995. Self-assembly in vitro of purified CA-NC proteins from Rous sarcoma virus and human immunodeficiency virus type 1. J. Virol. **69:**6487–6497.
11. **Cimarelli, A., S. Sandin, S. Hoglund, and J. Luban.** 2000. Basic residues in human immunodeficiency virus type 1 nucleocapsid promote virion assembly via interaction with RNA. J. Virol. **74:**3046–3057.
12. **Dannull, J., A. Surovoy, G. Jung, and K. Moelling.** 1994. Specific binding of HIV-1 nucleocapsid protein to PSI RNA in vitro requires N-terminal zinc finger and flanking basic amino acid residues. EMBO J. **13:**1525–1533.
13. **Darlix, J. L., M. Lapadat-Tapolsky, H. de Rocquigny, and B. P. Roques.** 1995. First glimpses at structure-function relationships of the nucleocapsid protein of retroviruses. J. Mol. Biol. **254:**523–537.
14. **Dawson, L., and X. F. Yu.** 1998. The role of nucleocapsid of HIV-1 in virus assembly. Virology **251:**141–157.
15. **Dorfman, T., J. Luban, S. P. Goff, W. A. Haseltine, and H. G. Gottlinger.** 1993. Mapping of functionally important residues of a cysteine-histidine box in the human immunodeficiency virus type 1 nucleocapsid protein. J. Virol. **67:**6159–6169.
16. **Dupraz, P., and P. F. Spahr.** 1992. Specificity of Rous sarcoma virus nucleocapsid protein in genomic RNA packaging. J. Virol. **66:**4662–4670.
17. **Embretson, J. E., and H. M. Temin.** 1987. Lack of competition results in efficient packaging of heterologous murine retroviral RNAs and reticuloendotheliosis virus encapsidation-minus RNAs by the reticuloendotheliosis virus helper cell line. J. Virol. **61:**2675–2683.
18. **Fisher, A. G., E. Collalti, L. Ratner, R. C. Gallo, and F. Wong-Staal.** 1985. A molecular clone of HTLV-III with biological activity. Nature **316:**262–265.
19. **Freed, E. O.** 1998. HIV-1 gag proteins: diverse functions in the virus life cycle. Virology **251:**1–15.
20. **Ganser, B. K., S. Li, V. Y. Klishko, J. T. Finch, and W. I. Sundquist.** 1999. Assembly and analysis of conical models for the HIV-1 core. Science **283:**80–83.
21. **Garnier, L., J. B. Bowzard, and J. W. Wills.** 1998. Recent advances and remaining problems in HIV assembly. AIDS **12**(Suppl. A)**:**S5–S16.
22. **Garnier, L., L. Ratner, B. Rovinski, S. X. Cao, and J. W. Wills.** 1998. Particle size determinants in the human immunodeficiency virus type 1 Gag protein. J. Virol. **72:**4667–4677.
23. **Gheysen, D., E. Jacobs, F. de Foresta, C. Thiriart, M. Francotte, D. Thines, and M. De Wilde.** 1989. Assembly and release of HIV-1 precursor Pr55gag virus-like particles from recombinant baculovirus-infected insect cells. Cell **59:**103–112.
24. **Giddings, A. M., G. D. Ritter, Jr., and M. J. Mulligan.** 1998. The matrix protein of HIV-1 is not sufficient for assembly and release of virus-like particles. Virology **248:**108–116.
25. **Gorelick, R. J., L. E. Henderson, J. P. Hanser, and A. Rein.** 1988. Point mutants of Moloney murine leukemia virus that fail to package viral RNA: evidence for specific RNA recognition by a "zinc finger-like" protein sequence. Proc. Natl. Acad. Sci. USA **85:**8420–8424.
26. **Hockley, D. J., M. V. Nermut, C. Grief, J. B. M. Jowett, and I. M. Jones.** 1994. Comparative morphology of Gag protein structures produced by mutants of the gag gene of human immunodeficiency virus type 1. J. Gen. Virol. **75:**2985–2997.
27. **Housset, V., H. De Rocquigny, B. P. Roques, and J. L. Darlix.** 1993. Basic amino acids flanking the zinc finger of Moloney murine leukemia virus nucleocapsid protein NCp10 are critical for virus infectivity. J. Virol. **67:**2537–2545.
28. **Jowett, J. B., D. J. Hockley, M. V. Nermut, and I. M. Jones.** 1992. Distinct signals in human immunodeficiency virus type 1 Pr55 necessary for RNA binding and particle formation. J. Gen. Virol. **73:**3079–3086.
29. **Kempf, D. J., K. C. Marsh, J. F. Denissen, E. McDonald, S. Vasavanonda, C. A. Flentge, B. E. Green, L. Fino, C. H. Park, X. P. Kong, et al.** 1995. ABT-538 is a potent inhibitor of human immunodeficiency virus protease and has high oral bioavailability in humans. Proc. Natl. Acad. Sci. USA **92:**2484–2488.
30. **Khan, M. A., C. Aberham, S. Kao, H. Akari, R. Gorelick, S. Bour, and K. Strebel.** 2001. Human immunodeficiency virus type 1 Vif protein is packaged into the nucleoprotein complex through an interaction with viral genomic RNA. J. Virol. **75:**7252–7265.
31. **Laemmli, U. K.** 1970. Cleavage of structural proteins during the assembly of the head of bacteriophage T4. Nature **227:**680–685.
32. **Lindwasser, O. W., and M. D. Resh.** 2001. Multimerization of human immunodeficiency virus type 1 Gag promotes its localization to barges, raft-like membrane microdomains. J. Virol. **75:**7913–7924.
33. **Lingappa, J. R., R. L. Hill, M. L. Wong, and R. S. Hegde.** 1997. A multistep, ATP-dependent pathway for assembly of human immunodeficiency virus capsids in a cell-free system. J. Cell Biol. **136:**567–581.
34. **Malim, M. H., J. Hauber, S. Y. Le, J. V. Maizel, and B. R. Cullen.** 1989. The HIV-1 rev trans-activator acts through a structured target sequence to activate nuclear export of unspliced viral mRNA. Nature **338:**254–257.
35. **McBride, M. S., and A. T. Panganiban.** 1996. The human immunodeficiency virus type 1 encapsidation site is a multipartite RNA element composed of functional hairpin structures. J. Virol. **70:**2963–2973.
36. **McBride, M. S., and A. T. Panganiban.** 1997. Position dependence of functional hairpins important for human immunodeficiency virus type 1 RNA encapsidation in vivo. J. Virol. **71:**2050–2058.
37. **Meric, C., and S. P. Goff.** 1989. Characterization of Moloney murine leukemia virus mutants with single-amino-acid substitutions in the Cys-His box of the nucleocapsid protein. J. Virol. **63:**1558–1568.
38. **Meric, C., E. Gouilloud, and P. F. Spahr.** 1988. Mutations in Rous sarcoma virus nucleocapsid protein p12 (NC): deletions of Cys-His boxes. J. Virol. **62:**3328–3333.
39. **Meric, C., and P. F. Spahr.** 1986. Rous sarcoma virus nucleic acid-binding protein p12 is necessary for viral 70S RNA dimer formation and packaging. J. Virol. **60:**450–459.
40. **Muriaux, D., J. Mirro, D. Harvin, and A. Rein.** 2001. RNA is a structural element in retrovirus particles. Proc. Natl. Acad. Sci. USA **98:**5246–5251.
41. **Naldini, L., U. Blomer, P. Gallay, D. Ory, R. Mulligan, F. H. Gage, I. M. Verma, and D. Trono.** 1996. In vivo gene delivery and stable transduction of nondividing cells by a lentiviral vector. Science **272:**263–267.
42. **Nascimbeni, M., C. Lamotte, G. Peytavin, R. Farinotti, and F. Clavel.** 1999. Kinetics of antiviral activity and intracellular pharmacokinetics of human immunodeficiency virus type 1 protease inhibitors in tissue culture. Antimicrob. Agents Chemother. **43:**2629–2634.
43. **Nguyen, D. H., and J. E. Hildreth.** 2000. Evidence for budding of human immunodeficiency virus type 1 selectively from glycolipid-enriched membrane lipid rafts. J. Virol. **74:**3264–3272.
44. **Poon, D. T., G. Li, and A. Aldovini.** 1998. Nucleocapsid and matrix protein contributions to selective human immunodeficiency virus type 1 genomic RNA packaging. J. Virol. **72:**1983–1993.
45. **Poon, D. T., J. Wu, and A. Aldovini.** 1996. Charged amino acid residues of human immunodeficiency virus type 1 nucleocapsid p7 protein involved in RNA packaging and infectivity. J. Virol. **70:**6607–6616.
46. **Rein, A.** 1994. Retroviral RNA packaging: a review. Arch. Virol. Suppl. **9:**513–522.
47. **Rein, A., D. P. Harvin, J. Mirro, S. M. Ernst, and R. J. Gorelick.** 1994. Evidence that a central domain of nucleocapsid protein is required for RNA packaging in murine leukemia virus. J. Virol. **68:**6124–6129.
48. **Rein, A., L. E. Henderson, and J. G. Levin.** 1998. Nucleic-acid-chaperone activity of retroviral nucleocapsid proteins: significance for viral replication. Trends Biochem. Sci. **23:**297–301.
49. **Sandefur, S., V. Varthakavi, and P. Spearman.** 1998. The I domain is required for efficient plasma membrane binding of human immunodeficiency virus type 1 $Pr55^{Gag}$. J. Virol. **72:**2723–2732.
50. **Schmalzbauer, E., B. Strack, J. Dannull, S. Guehmann, and K. Moelling.** 1996. Mutations of basic amino acids of NCp7 of human immunodeficiency virus type 1 affect RNA binding in vitro. J. Virol. **70:**771–777.
51. **Swanstrom, R. W., and J. W. Wills.** 1997. Synthesis, assembly and processing of viral proteins, p. 263–334. *In* J. M. Coffin, S. H. Hughes, and H. E. Varmus (ed.), Retroviruses. Cold Spring Harbor Laboratory Press, Plainview, N.Y.
52. **Tritel, M., and M. D. Resh.** 2000. Kinetic analysis of human immunodeficiency virus type 1 assembly reveals the presence of sequential intermediates. J. Virol. **74:**5845–5855.
53. **Wang, C. T., H. Y. Lai, and J. J. Li.** 1998. Analysis of minimal human immunodeficiency virus type 1 Gag coding sequences capable of virus-like particle assembly and release. J. Virol. **72:**7950–7959.
54. **Zhang, Y., and E. Barklis.** 1995. Nucleocapsid protein effects on the specificity of retrovirus RNA encapsidation. J. Virol. **69:**5716–5722.
55. **Zhang, Y., H. Qian, Z. Love, and E. Barklis.** 1998. Analysis of the assembly function of the human immunodeficiency virus type 1 Gag protein nucleocapsid domain. J. Virol. **72:**1782–1789.